Use of An Equivalent Thermal Network For The Analysis of a Coupled Thermo-Magnetic problem

FRANCESCO DELLA TORRE, SONIA LEVA, ADRIANO PAOLO MORANDO
Energy Department
Politecnico di Milano
Piazza Leonardo da Vinci, 32 – 20133 Milano
ITALY
francesco.dellatorre, sonia.leva, adriano.morando@polimi.it

Abstract: - The coupled magneto-thermal problem is analyzed, with reference to a particular heating application, by means of an equivalent thermal network, that is based on a first-approximation interpretation of the field equations. The connections between the thermal characteristics and the magnetic ones are taking into account by considering the skin-effect and the dependence of electric conductibility on the temperature. Also the dependence of the produced heat – by Joule effect – on frequency is taken into account.
A specific and straightforward applicative case is analyzed in order to underline the validity and the advantages of the proposed model. A single conductive loop is lighting by an impressed perpendicular magnetic field and both the forward and inverse problems are analyzed.
An integration technique, based on Matlab-Simulink, is shown for the solution of the problem. Moreover, the dependence of the achieved results on the geometric characteristics of the analyzed system is studied.

Key-Words: - Electroheat applications, Coupled thermo-magnetic problem, Numerical method, Thermal network

1 Introduction

The coupled thermo-magnetic problem plays a fundamental role in several applications of the engineering science. For example, it is very important for the operation of electrical rotating machines, especially for induction-cage motor [1] and permanent-magnet machines [2]

Moreover, it is very important for the calculation of the equivalent electrical parameters (typically: resistances and inductances) of conductors, for example in a transmission line propagation problems [3]. Furthermore it plays the main role in electromagnetic heating applications process [4]: induction heating is widely used in industrial applications, e.g. heat treatment of metals, forging, surface hardening, where the knowledge of the induced power density and transient temperature distributions are of fundamental importance for the required technological result.

Nowadays several packages based on numerical methods are available for the solution of eddy current and thermal problems. The principals of them are: Finite Difference methods [5], Boundary Elements methods [6], Finite Elements Analysis [7] and derived methods [8], and, finally, the more recent cell method [9]. A critical collection of some of these methods can be founded in [10].

In spite of this, the prediction of the power density distributions and the temperature profile is relatively complex because the electromagnetic and thermal problems are coupled and both problems are non linear since the electrical and magnetic properties of the material are strongly temperature dependent and - in several ferromagnetic materials - the permeability is also a function of the local magnetic field intensity.

Furthermore, all the developed numerical techniques have in common the difficult to formulate analytically the problem, the big cost in terms of CPU time and memory capacity required, and the not easy interpretation of the obtained results.

In the present paper a first-approximation method is proposed to solve the electromagnetic-thermal problems with reference to a particular heating application, firstly analyzed in scientific paper. The proposed technique is based on the numerical solution of a thermal equivalent network.

The obtained results can be easily used to determine the convenience of improving more detailed numerical calculus in order to design the device under study.

2 Problem Formulation

The whole coupled electromagnetic-thermal problem can be described, using the magnetic vector potential $\bar{A}$ and the scalar electric potential v and considering, for the sake of simplicity, time-harmonic fields with the following well-known set of equations [11]-[12]:

$$\begin{cases} \frac{1}{\mu(T)}\nabla\times(\nabla\times\bar{A}) - \frac{1}{\mu(T)}\nabla(\nabla\cdot\bar{A}) + \\ \qquad + j\omega\varepsilon(T)(\bar{A}+\nabla v) = \bar{J} \\ c_p\gamma\frac{\partial T}{\partial t} - k\nabla\cdot(\nabla T) = q \end{cases} \quad (1)$$

where μ is the magnetic permeability, T is the absolute temperature, c_p is the specific heat at constant pressure, k is the thermal conductivity, q is the heat source and $\bar{J}$ is the current density.

Observing that:

$$\begin{cases} \bar{J} = \sigma(T)\bar{E} = \frac{\sigma_0}{1+\alpha(T-T_0)}\bar{E} \\ q = \sigma(T)E^2 \end{cases} \quad (2)$$

where σ is the electric conductivity, α the temperature coefficient and the subscript "0" indicates the reference temperature (for example, the environment one), it is possible to conclude that the problem is nonlinear.

In fact, the electromagnetic characteristics are dependent on temperature T, time t, the position in the considered space and, as regards the magnetic permeability, also on magnetic field intensity. For this reason, even if the electromagnetic equation is solved at a fixed temperature, when a magnetic material is present in the solution domain the equation becomes non linear.

Also thermal problem is non linear both for the material properties dependence on temperature and non linear boundary conditions. Moreover, the temperature depends on the impressed heat that depends on the electric field and, by means of eddy currents, also on the magnetic one.

The electromagnetic and thermal problems are represented by the non linear partial differential equation system constituted by (1) and (2). Its analytical solution is practically impossible, especially when the system configuration is geometrically complex.

An approximate solution of the electromagnetic and thermal problems have to be developed overall if the technical problem is for the first time analyzed. A first-order solution can be developed by means of equivalent thermal network: it will be shown in the next section.

3 Thermal equivalent network formulation of the analyzed problem

The thermal problem under study concern the possibility to reach high temperature in a texture made of steel. The temperature have to be sufficient to weld loops between them without damage the texture itself. The texture will be considerate all made by the same material and the induced field uniformly distributed in the space. In this condition, the emf induced by the speed of the texture is equal to zero.

In order to verify the achieved temperature, its connection with the characteristic of the induced field and to show the proposed method, the base element of the texture can be analyzed. It is a single steel building block with square section.

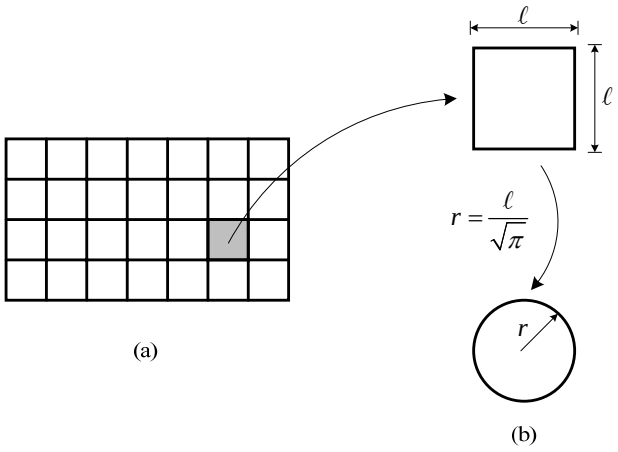

Fig. 1. The analyzed steel texture (a) and its basic element (b). The equivalence between the square basic element and the circular one is also reported.

In order to simplify the approach, it is possible to consider, as it is shown in fig. 2, an equivalent circular loop whit radius r. In the same figure the relation that allow the calculation of this radius is still reported.

The circular loop is dipped in a time-harmonic uniformly distributed magnetic field and it is sketched in fig. 2. The unit vector $\vec{n}$ is normal to the surface S, that has the loop as a border; it is supposed to be parallel to the magnetic field lines of force.

The impressed magnetic field is time-harmonic and can be expressed as follows:

$$b(t) = \sqrt{2}B\cos(\omega t) \quad (3)$$

its time derivative is:

$$\frac{db(t)}{dt} = -\sqrt{2}\omega B\sin(\omega t) \quad (4)$$

consequently the Faraday's law for the loop gives:

$$e(t) = \sqrt{2}SB\omega\sin(\omega t) \quad (5)$$

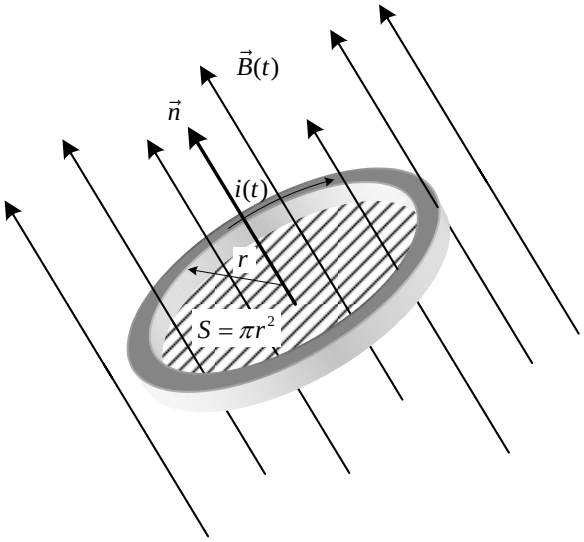

Fig. 2. Details of the equivalent circular loop of fig. 1-b.

This electromotive force causes the flow of the following current into the loop:

$$i(t) = \sqrt{2}\frac{e(t)}{R}\sin(\omega t) = i(t) = \sqrt{2}\frac{SB\omega}{R}\sin(\omega t) \quad (6)$$

Starting from the rms value B and the angular frequency ω of the impressed magnetic field and assuming that the resistance of the loop is constant, eq. (6) allows the calculation of this current.

The current i(t) imposes an heating process to the loop; this process can be studied by means of the equivalent thermal network shown in fig. 3. The impressed heat source is:

$$q(t) = Ri(t)^2 \quad (7)$$

The lumped thermal parameters (conductance G and capacitance C) have the following expression:

$$\begin{cases} G = k \cdot \dfrac{\Sigma}{2\pi r} = k \cdot \dfrac{\rho^2}{2\pi r} \\ C = m \cdot c_p = \gamma V c_P = \gamma 2\pi^2 \rho^2 r c_p \end{cases} \quad (8)$$

where m is the mass of the loop and ρ is the radius of the transversal section Σ of the wire.

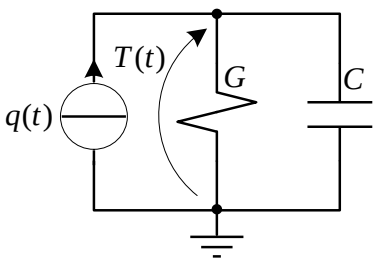

Fig. 3. The equivalent thermal network with constant lumped elements used for the analysis of the magneto-electric process to which the loop in Fig. 2 is subjected.

Parameter	Symbol	Value	Measure unit
Specific weight	γ	7900	$\frac{kg}{m^3}$
Specific heat	c_p	500	$\frac{J}{kg \cdot K}$
Thermal conductivity	k	44.5	$\frac{W}{m \cdot K}$
Electric conductibility a 20 °C (293,15 K)	σ_0	73×10^4	$\frac{S}{m}$
Relative magnetic permeability	μ_R	1,1	[−]
Temperature coefficient	α	0.0045	$\frac{1}{K}$

Table. 1. Characteristics of EN.4301-AISI 304 steel.

4 Thermal and electromagnetic parameters dependence on frequency and temperature

It is well-known that the value of the resistance of a conductor is affected by the skin-effect [11]. If the resistance calculated on stationary conditions (for a nil value of the frequency f) is:

$$R_{DC} = \rho\frac{2\pi r}{\Sigma} = \frac{1}{\sigma}\cdot\frac{2r}{\rho^2} \quad (9)$$

then the equivalent resistance calculated for the generic value of the frequency is:

$$R(f) = R_{DC}\cdot K_{se}(f) \quad (10)$$

where $K_{se}(f)$ is the skin-effect factor:

$$K_{se}(f) = \frac{\rho^2}{\left[\rho - \delta(f)\right]^2} \quad (11)$$

and $\delta(f)$ is the skin-depth:

$$\delta(f) = \frac{1}{\sqrt{\pi f \mu \sigma}} \quad (12)$$

Moreover, because the electric conductibility depends on the temperature (see the first of (2)), the resistance R_{DC}, the skin-dept and the skin-effect factor also depend on it. Basing on this consideration, the (10) becomes:

$$R(f,T) = \frac{2r}{\dfrac{\rho^2\sigma_0}{1+\alpha(T-T_0)} + \dfrac{1}{\pi f \mu} - 2\rho\sqrt{\dfrac{1}{\pi f \mu}\cdot\left[\dfrac{1+\alpha(T-T_0)}{\sigma_0}\right]^3}} \quad (13)$$

As an example, it is possible to consider a loop constituted of EN.4301-AISI 304 steel, which characteristics are reported in Table 1. In fig. 4 the graph

of the dependence of R_{DC} on the temperature T is reported. In fig. 5 and fig. 6 are also sketched, respectively, the skin-effect factor $K_{se}(f,t)$ and the equivalent resistance $R(f,t)$ of the loop.

Also the thermal lumped parameters in fig. 3 depend on the temperature. By first approximation, it is possible to consider as negligible these dependences.

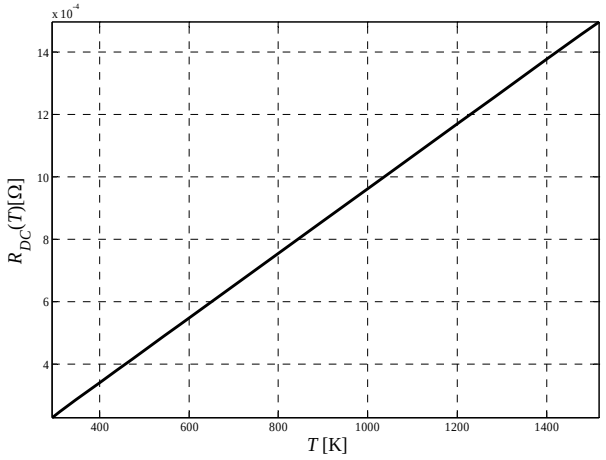

Fig. 4. Dependence on T of the resistance R_{DC}.

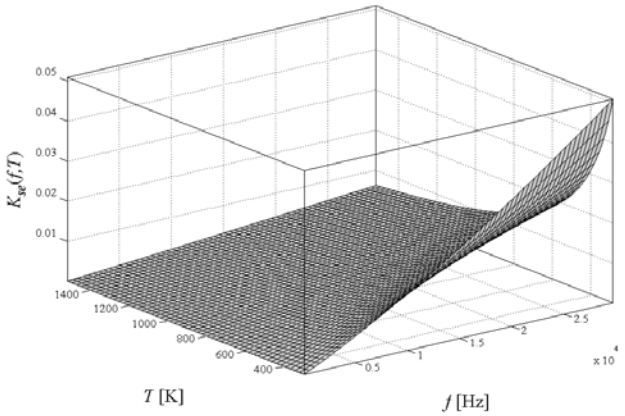

Fig. 5. Dependence on f and T of the skin-effect factor.

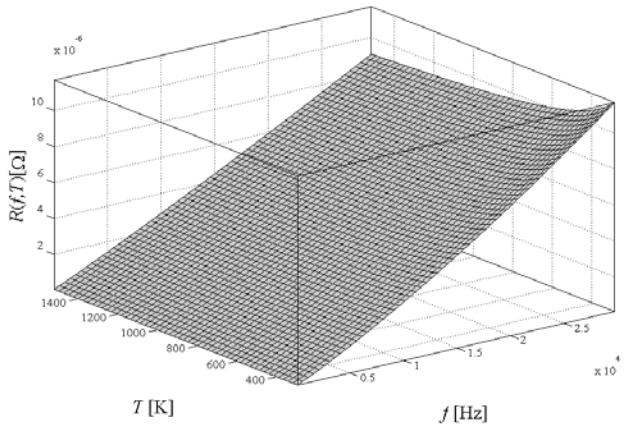

Fig. 6. Dependence on f and T of the equivalent resistance of the considered loop.

4 Formulation of the whole problem

Thanks to the previous considerations, it is clearly shown that, as a matter of fact, the nonlinear problem under study presents a strictly interlink between its thermal and electromagnetic aspects. This fact can be also observed in the whole thermal-electromagnetic formulation (1)-(2).

Consequently the thermal equivalent network depends on the electromagnetic characteristics of the impressed field and, also, these characteristics depend on the thermal process.

The first-order differential equation that solves the equivalent thermal network is:

$$q = GT + C\frac{dT}{dt} \tag{14}$$

Considering eq. (7), the (13) becomes:

$$R(f,T)i(t)^2 = GT(f,t) + C\frac{dT(f,t)}{dt} \tag{15}$$

and, substituting eq. (13):

$$\frac{2ri(t)^2}{\dfrac{\rho^2\sigma_0}{1+\alpha\left(T-T_0\right)} + \dfrac{1}{\pi f\mu} - 2\rho\sqrt{\dfrac{1}{\pi f\mu}\cdot\left[\dfrac{1+\alpha\left(T-T_0\right)}{\sigma_0}\right]^3}} = GT(f,t) + C\frac{dT(f,t)}{dt} \tag{16}$$

Substituting the current with its expression (6), we obtain:

$$\frac{16r^3B^2\pi^3f^2}{\dfrac{\rho^2\sigma_0}{1+\alpha\left(T-T_0\right)} + \dfrac{1}{\pi f\mu} - 2\rho\sqrt{\dfrac{1}{\pi f\mu}\cdot\left[\dfrac{1+\alpha\left(T-T_0\right)}{\sigma_0}\right]^3}} \times\frac{\sin^2\left(2\pi ft\right)}{R(f,T)^2} = GT(f,t) + C\frac{dT(f,t)}{dt} \tag{17}$$

Replacing the expression (13) for the resistance, it follows:

$$4rB^2\pi^3f^2\left\{\frac{\rho^2\sigma_0\pi f\mu + 1 + \alpha\left(T-T_0\right)}{\left[1+\alpha\left(T-T_0\right)\right]\pi f\mu} - 2\rho\sqrt{\frac{1}{\pi f\mu}\cdot\left[\frac{1+\alpha\left(T-T_0\right)}{\sigma_0}\right]^3}\sin^2\left(2\pi ft\right)\right\} = GT(f,t) + C\frac{dT(f,t)}{dt} \tag{18}$$

Considering the expressions (8) for the thermal parameters, the previous becomes:

$$\frac{\rho^2\sigma_0\pi f\mu+1+\alpha(T-T_0)}{\left[1+\alpha(T-T_0)\right]\pi f\mu}$$
$$-2\rho\sqrt{\frac{1}{\pi f\mu}\cdot\left[\frac{1+\alpha(T-T_0)}{\sigma_0}\right]^3}\sin^2(2\pi ft)$$
$$=\frac{k\rho^2}{8r^2B^2\pi^4f^2}T(f,t)+\frac{\gamma\rho^2c_p}{2B^2\pi f^2}\frac{dT(f,t)}{dt} \quad (19)$$

Rearranging and expressing the (19) in the normal form, it is finally obtained:

$$\frac{dT(f,t)}{dt}+\frac{k}{4\gamma c_p r^2\pi^3}T(f,t)$$
$$-\frac{2B^2f}{\gamma\mu\rho^2c_p}\cdot\frac{\rho^2\sigma_0\pi f\mu+1+\alpha(T-T_0)}{\left[1+\alpha(T-T_0)\right]}$$
$$+\frac{4B^2\pi f^2}{\gamma\rho c_p}\sqrt{\frac{1}{\pi f\mu}\cdot\left[\frac{1+\alpha(T-T_0)}{\sigma_0}\right]^3}\sin^2(2\pi ft)=0 \quad (20)$$

The nonlinear first-order differential equation (20) represents the proposed model. Its numerical solution will be treated in the next section.

5 Numerical integration of the model

Due to the strictly linkage between electromagnetic and thermal characteristics and to the nonlinearity of the obtained equations, the integration of the complete model can be necessarily obtained by means of a numerical approach.

The proposed model can be used for the forward problem (giving *B* and *f*, obtaining T(t)) or for the inverse model (giving the wished final T_{ref}, determining the field that imposed it). Both two problems can be sketched with a block diagram, as it is shown in fig. 7 and fig. 8.

The numerical algorithm for the solution is implemented with Matlab-Simulink. In fig. 9 the considered total Simulink block diagram is shown. The block named "Loop" is the core of the algorithm, as it represent the eq. (20).

In order to allow an easily change of the parameter of the magneto-thermal system, we have provided a mask for this block, reported in fig. 10. With the use of this mask, the user can change the numerical values of the indicated parameters. The block "Loop" is composed by others Simulink blocks, that are shown in fig. 11.

The block named "R_DC", shown in fig. 12, implement the expression of the resistance of the loop calculated for $f = 0$, in base on eq. (9).

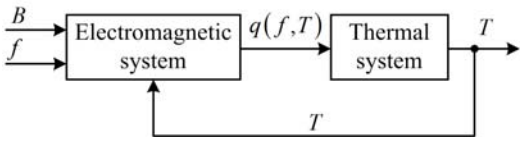

(a)

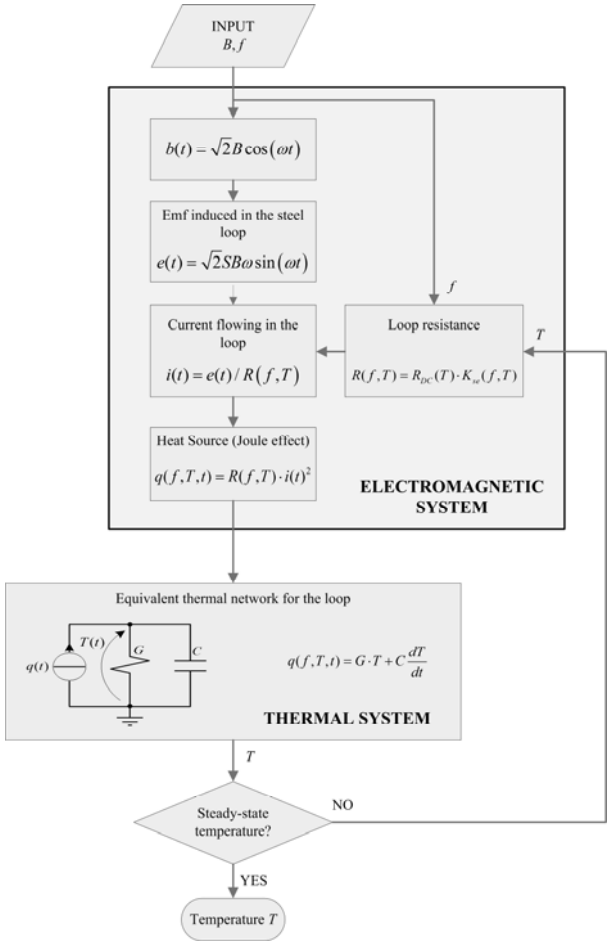

(b)

Fig. 7. Block diagram for the forward problem: (a) general diagram; (b) complete diagram.

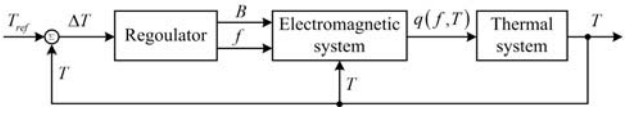

Fig. 8. Block diagram for the inverse problem.

In order to obtain the resistance of the loop for every values of frequency and temperature, the output of the block "R_DC" is multiplied with the output of the block named "Kse(f,t)", that implement the calculus of the skin effect factor (11), also considering the skin depth (12). The block "Kse(f,t)" is represented in fig. 13 .

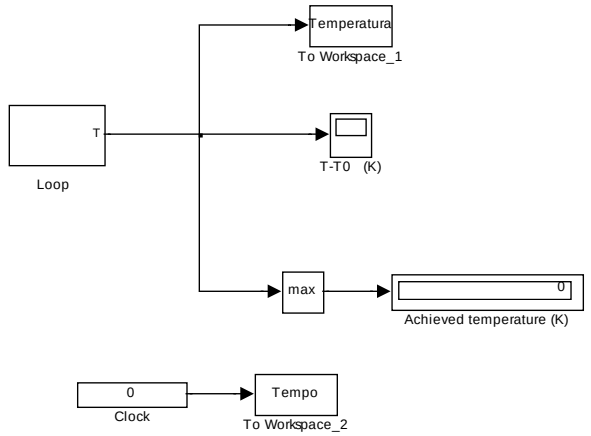

Fig. 9. Total Matlab-Simulink diagram used for the numeric simulations.

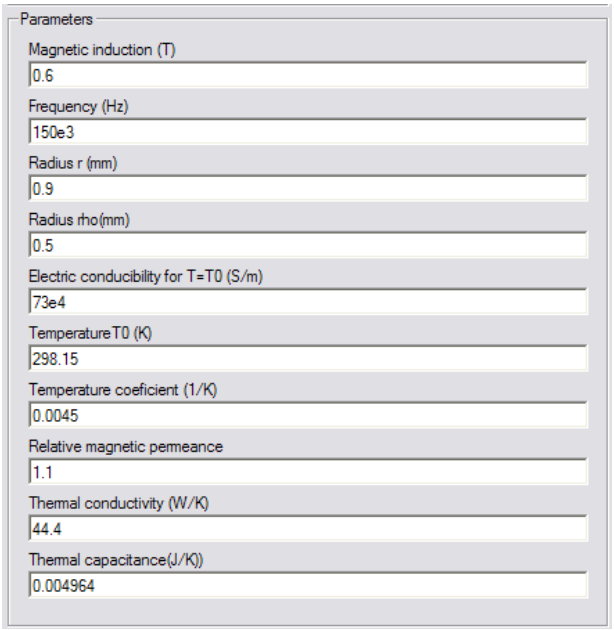

Fig. 10. Mask for the insertion of the physical parameters of the Matlab-Simulink model.

Both the blocks "R_DC" and "Kse(f,t)" need as input the different values of σ. These values are obtained with the block named "Sigma", that has in input the current value of temperature. This block is sketched in fig. 14 and it is implemented in base on the first of (2).

The last block, shown in fig. 15, represents the thermal network with lumped elements, just sketched in fig. 2. As Simulink need the use of Laplace Transformation, eq. (14), that represent the thermal network, is transformed in a transfer function in this domain. Applying Laplace Transformation, the (14) becomes:

$$q(s) = GT(s) + CsT(s) = (G + sC)T(s) \qquad (21)$$

So the link between the input power – that is due to Joule effect – and the output temperature is:

$$T(s) = \frac{1}{G + sC} q(s) \qquad (22)$$

This equation expresses the thermal transfer function that is the core of the block "thermal network".

It is important to note that Laplace Transformation requires that the analyzed system is linear [14], so it is no formally applicable to the considered problem. But Simulink allows the use of Laplace Transformation also for nonlinear system; so there are no problem if, as in the considered study, the problem is nonlinear.

7 Numeric examples

Using the proposed procedure and the numerical integration described in the previous section, we have studied both the forward and the inverse problem.

In fig. 16 the solution of the forward problem is graphically shown; the diagram reports the temperature values obtained varying the rms B and the frequency f of the applied field. From this graph it is clear that greater are induction and frequency, greater is the achieved temperature.

In order to exhibit the use of the proposed model for the solution of inverse problem, the numeric software is utilized to determine the optimum values of B and f in order to achieve the wished temperature of 1473.15 K. The geometric characteristics of the loop are: r=0.8 mm, ρ=0.1 mm. In fig. 17 the transient of the temperature is reported for different value of B and f.

As it is possible to observe from these graphs, knowing the whished value of temperature T_{ref} the possible values of B and f that allows its attainment are more than one. The choice between them of the best values requires to know in depth the technology of construction of the machines that generate the impressed magnetic field.

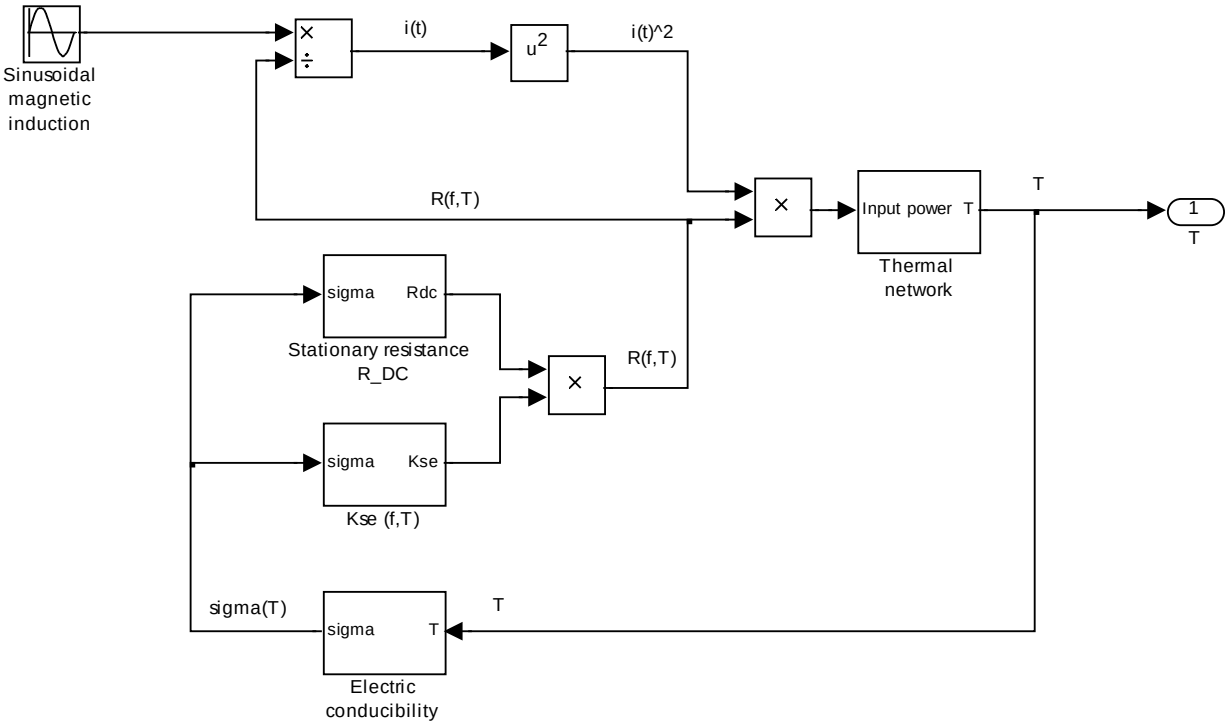

Fig. 11. Electro-thermal Matlab-Simulink total model.

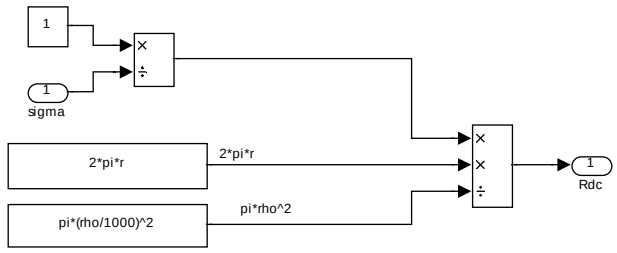

Fig. 12. Simulink block "R_DC".

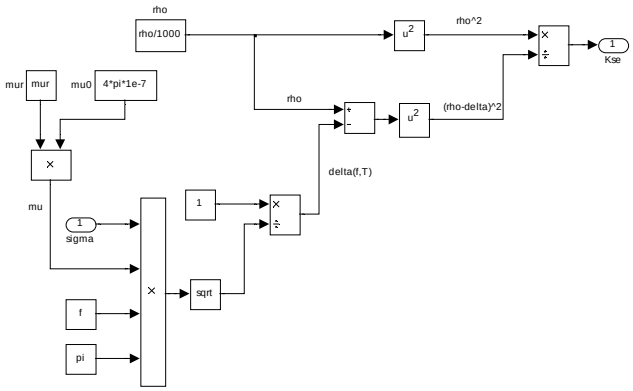

Fig. 13. Simulink block "Kse(f,t)".

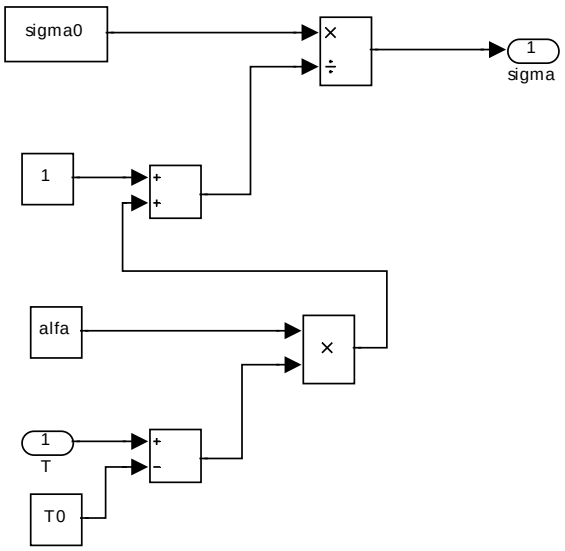

Fig. 14. Simulink block for the calculation of the eelectric conductibility of the loop.

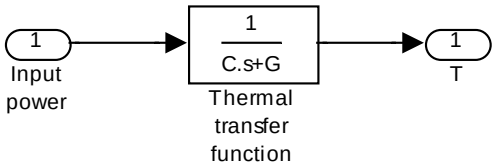

Fig. 15. Simulink block that represent the equivalent tthermal network of fig. 2.

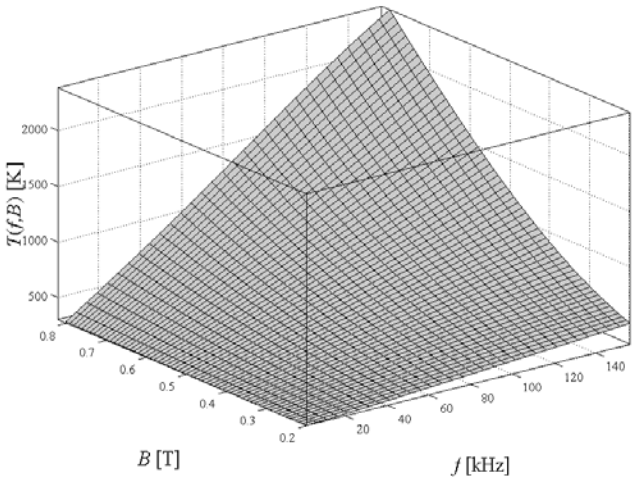

Fig. 16. Example of the solution of the forward problem.

8 Variation of the achieved temperature with dimensions of the loop

It is also interesting to analyze the influence of the geometry of the considered loop on the achieved temperature.

Considering the case just analyzed (see the first diagram in fig. 17), we maintain constant the rms value of the magnetic induction B of and the value of the frequency f and we can varying the radii r of the equivalent circular loop and ρ of the transversal section of the steel wire. The obtained result are reported in fig. 18 and fig. 19. These graphs illustrate the different achieved temperatures for different values of r and ρ.

These results show that greater are the radii r and ρ, bigger is the achieved temperature. As a result if it is possible to design ex-novo the texture, it is preferable to choose the largest square dimensions allowed by other project bonds. Furthermore, the values of B and f that allow the attainment of temperature T_{ref} are diverse considering different size of steel texture. The proposed analysis can give some indication for each considered case.

6 Conclusion

In this paper a first-order model has been presented to study the possibility to reach high temperature in a texture made of steel by means of electromagnetic heating process.

The electromagnetic and thermal problems are represented by non linear partial differential equations: they are affected by intrinsic nonlinearity due to the skin effect and to the strongly dependence of electrical and magnetic properties on temperature. Its analytical solution is practically impossible, for these reasons, a first order approximate model and its numerical integration are necessary, overall if the problem is analyzed for the first time. In the paper an example of first-order approximate solution is presented, based on the use of MatLab-Simulink.

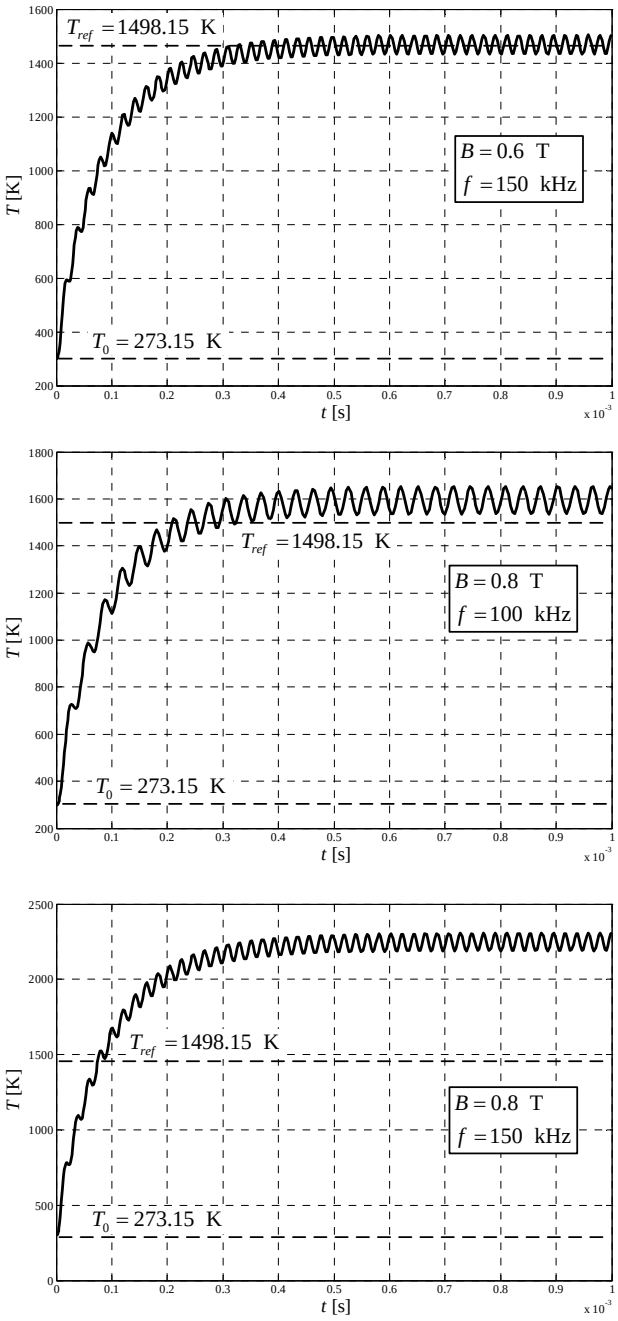

Fig. 17. Transient of the temperatures obtained with different values of B and f.

By means of the proposed model and of the numerical integration, both the forward and inverse problems are considered. With reference to a specific example it has been shown that the model allows the resolution of the two type of problem,

which results would have been interpreted with adjunctive considerations based on the knowledge of the technology by which the external magnetic field can be impressed to the considered system.

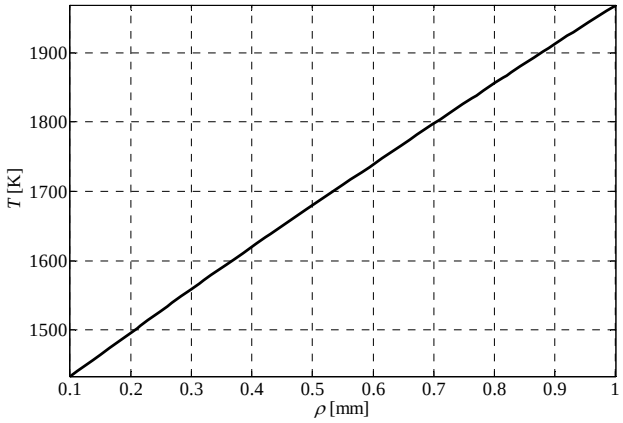

Fig. 18. Variation of the steady-state temperature with the radius ρ of the transversal section of the steel wire at B=0.6 T and f=150kHz.

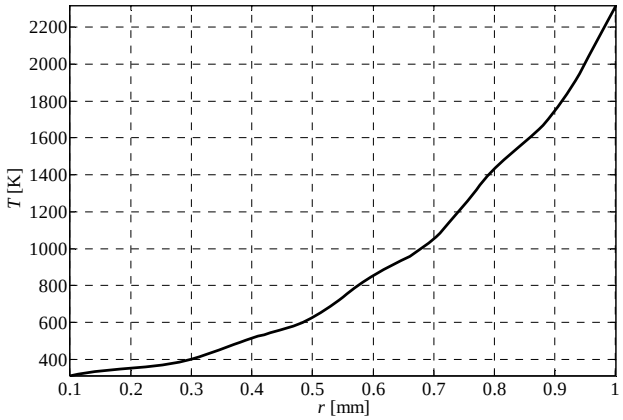

Fig. 19. Variation of the steady-state temperature with the radius r of the equivalent circular loop at B=0.6 T and f=150kHz.

Further developments will necessary consider not only one constitutive element of the texture in a uniformly distributed field but the complete texture in the real field. Consequently, the characteristic of the machines that generate the impressed magnetic field will be take into consideration. Finally, the dependence of the magnetic permeability and of the lumped parameters in the equivalent thermal network on temperature will be also taking into account.

References:

[1] Z. J. Liu, K. J. Binns, and T. S. Low, Analysis of Eddy Current and Thermal Problems in Permanent Magnet Machines with Radial-Field Topologies, *IEEE Transaction on Magnetics*, Vol. 31, No. 3, May 1995, pp. 1912-191

[2] M. Liwschitz, and C. C. Whipple, *Electric Machinery, AC Machines*, D. Van Nostrand Company, Princeton, 1946

[3] M. A. R. Pozueta, L. F. M. Peñalba, and J. R. L. Diaz, Temperature factor for the accurate calculation of LV cables, *WSEAS Transaction on Circuit and Systems*, Vol. 4, No. 9, Sept. 2005, p. 1112

[4] S. Sharifian Attarl, M. C. E. Yagoub, and F. Mohammadi, Simulation of Electro-Thermal Effects in Device and Circuit, *WSEAS Transaction on Circuits and Systems*, Vol. 5, No. 7, July 2006, p. 926

[5] D. Zabala, and A. L. L. De Ramos, Effect of the Finite Difference Solution Scheme in a Free Boundary Convective Mass Transfer Model, *WSEAS Transaction on Mathematics*, Vol. 6, No. 6, June 2007, p. 693

[6] A. Mühlbauer, A. Muiznieks, and H. J. Leßmann, The Calculation of 3D High-Frequency Electromagnetic Fields During Induction Heating Using the BEM, *IEEE Transaction on Magnetics*, Vol. 29, No. 2, March 1993, pp. 1566-1569

[7] M. Lohakan, A Computational Model of Magnetic Fluid Flow using Maxwell's Equations, Heat Equations and Navier-Stokes Equations, *Proc. of 8th WSEAS Int. Conf. on Mathematical Methods and Computational Techniques in Electrical Engineering*, Bucharest, October 16-17, 2006, Paper No. 518-345, pp. 234-239

[8] I. C. Popa, I. Cautil, and D. Floricau, Electro-Thermal Numerical Model for Optimization of High Currents Dismountable Contacts, *Proc. of 8th WSEAS Int. Conf. on Mathematical Methods and Computational Techniques in Electrical Engineering*, Bucharest, October 16-17, 2006, Paper No. 518-381, pp. 103-106

[9] M. Bullo, F. Dugherio, M. Guarnieri, and E. Tittonel, Nonlinear Coupled Thermo-Electromagnetic Problems With the Cell Method, *IEEE Transaction on Magnetics*, Vol. 42, No. 4, Apr. 2006, pp. 991-994

[10] J. D. Lavers, Numerical Solution Methods For Electroheat Problems, *IEEE Trans. Magn.*, Vol. MAG-19, No. 6, Nov. 1983, pp. 2566-2572

[11] J. A. Lopez Molina, and M. Trujillo, Thermal Stresses in an Infinitely Long Solid Cylinder Using Green's Function and the Hyperbolic Heat Equation, *Proc. of the 2nd WSEAS Int. Conf. on Applied and Theoretical Mechanics*, Venice, Italy, November 20-22, 2006, Paper No. 539-233, pp. 63-67

[12] F. P. Incropera, D. P. DeWitt, *Fundamentals of*

heat and mass transfer, 4th ed., John Wiley & Sons., New York, 1996

[13] C. B. Moler, *Numerical computing with MATLAB*, SIAM, Philadelphia, 2004

[14] G. Doetsch, *Introduction to the Theory and Application of the Laplace Transformation*, Springer-Verlag, Berlin, 1974

[15] R. De Carlo, and P. M. Lin, *Linear Circuit Analysis: Time Domain, Phasor, and Laplace Transform Approaches*, 2nd ed., Oxford University Press, 2001